Polybutylene adipate terephthalate (PBAT) composites for thermally conductive, fire retardant, high dielectric applications using BaTiO$_3$ and MWCNTs as fillers

Eyob Wondu [a], Geunhyeong Lee [b], Jooheon Kim [a,b,c,*]

[a] Department of Intelligent Energy and Industry, Chung-Ang University, Seoul, 06974, Republic of Korea
[b] School of Chemical Engineering and Material Science, Chung-Ang University, Seoul, 06974, Republic of Korea
[c] Department of Advanced Materials Engineering, Chung-Ang University, Anseong-si, Gyeonggi-do, 17546, Republic of Korea

A B S T R A C T

This study provides a comprehensive investigation of the fabrication of novel composite materials by blending polybutylene adipate terephthalate (PBAT) with barium titanate (BaTiO$_3$) and multiwalled carbon nanotube (MWCNT) fillers. Prior to fabricating the composites, the filler surface treatments were tailored to enhance their compatibility with the PBAT matrix. Adipic acid (AA), a monomer for PBAT, was employed on the surface of the BaTiO$_3$ particles, while butanediol (BD) also a monomer of PBAT was used to modify the surface of the MWCNTs to ensure effective interaction with the PBAT chains during the composite fabrication process. The composite samples were produced by melt-blending at 140 °C, followed by injection molding at the same operating temperature for subsequent analysis. The results revealed remarkable improvements in the dielectric constant, thermal conductivity, fire retardancy, and tensile strength of the 40 wt% BaTiO$_3$ and MWCNT-PBAT blends compared to pure PBAT. The incorporation of BaTiO$_3$ additionally contributed to enhanced fire retardancy, mechanical properties, and dielectric properties, making the composite material more resistant to ignition and flame spread, thus rendering it suitable for applications requiring elevated fire safety. In addition, the inclusion of MWCNT improved thermal conductivity, enabling promising and efficient heat dissipation in various applications.

1. Introduction

The continuous drive for miniaturization in electrical and power systems has led to growing interest in developing compact materials with superior energy storage and efficient heat dissipation capabilities [1–6]. Among the various materials under investigation, electrostatic capacitors have emerged as a favorable choice owing to their rapid charge–discharge characteristics, reduced dielectric losses, and ability to withstand strong electronic fields. Capacitors have a wide range of applications in power supplies, defibrillators, actuators, inverters in electric vehicles, pulse networking, and electronic packaging. To meet the ever-evolving demands of such applications, efforts are required to enhance these materials' dielectric properties and thermal conductivities [2,7–12].

Polymer materials are widely utilized in dielectric and heat-dissipation applications because of their cost-effectiveness, lightweight nature, and flexibility. However, their inherent limitations, such as low dielectric constants and thermal conductivities, pose challenges to their effective utilization in high-performance applications [5,13, 14–21, 22–26]. To address these limitations, researchers have explored incorporating various filler materials into polymer matrices to enhance their properties. L. Zhao et al. proposed a solution for this by utilizing epoxy with SiC nanoparticles and BN to enhance the dielectric property and thermal conductivity. They coated the surface of SiC nanoparticles with SiO2 and prepared the hybrid filler with BN and obtained a dielectric constant of 8.19 and 0.72 W/(m.K) of thermal conductivity [20]. T. Taha et al. investigated the dielectric and thermal stability of PVA by incorporating SrTiO$_3$ and increased the dielectric constant and thermal stability [27].

Notably, barium titanate (BaTiO$_3$) and multiwalled carbon nanotubes (MWCNTs) have shown promise for significantly improving the dielectric constant and thermal conductivity of polymer composites.

The surfaces of $BaTiO_3$ and MWCNTs can be improved through suitable surface treatments to enhance their dispersion and compatibility within the polymer matrix. The crystal structure of $BaTiO_3$ enables the accumulation of electric charges at the interface between the medium and the polymer material [7,28] [–] [30], leading to a higher polarization density and improved dielectric constant. However, MWCNTs exhibit excellent thermal conductivity, rendering them a compelling choice for enhancing heat dissipation in polymer composites.

Considering the increasing demand for advanced polymer composites, developing materials with enhanced fire-retardant properties is imperative to ensure safety in electronic applications [31–33]. Therefore, the current study focused on improving the thermal conductivity, dielectric properties, and fire retardancy of PBAT composites by incorporating $BaTiO_3$ and MWCNTs, with particular emphasis on optimizing their surface properties.

PBAT, a thermoplastic polyester, has garnered significant attention owing to its excellent mechanical properties, including high flexibility, toughness, and elasticity and its biodegradable nature [32,34]. However, like many other polymer materials, PBAT exhibits limitations in terms of its thermal conductivity and dielectric properties [3,6,35,36]. Researchers have explored various approaches to address these challenges, such as incorporating filler materials into the polymer matrix. $BaTiO_3$, which exhibits a high dielectric constant owing to its crystal structure, has shown considerable potential for enhancing the dielectric properties of polymer composites. Moreover, MWCNTs, with exceptional thermal conductivity, have emerged as an attractive option for improving heat dissipation in polymer composites.

In this study, we investigated the fabrication of polymer composites via melt blending and low-speed melt extrusion by employing appropriate surface treatments to enhance the dispersion and compatibility of fillers within the PBAT matrix. By incorporating $BaTiO_3$ and MWCNTs, we aimed to develop a multifunctional polymer composite with improved thermal conductivity, dielectric properties, and fire retardancy, making it a promising candidate for various electronic applications. The focus of this study is to achieve an overall improvement in the thermal conductivity, dielectric properties, and fire retardancy of PBAT composites by combining the benefits of $BaTiO_3$ and MWCNTs and optimizing their surface properties. The resulting multifunctional polymer composites are expected to exhibit significant improvements in their critical properties, making them highly suitable for various electronic applications.

This study contributes to the field of advanced polymer composites by addressing the challenges posed by the inherently low thermal conductivity, poor dielectric properties, and fire retardancy of PBAT.

2. Experimental

2.1. Materials

The thermoplastic polymer PBAT was supplied by Dong-Sung Chemical, Ulsan, Korea. Acetone, oxalic acid anhydrous (OHA) were acquired from Dae-Jung Chemical and Metal Co., Ltd. (Seoul, Korea). Barium titanate ($BaTiO_3$; 10 μm, 99 %) was procured from Alfa Aesar (USA). MWCNTs, tetrabutoxytitanium, and adipic acid (AA) were acquired from Sigma-Aldrich (St. Louis, MI, USA).

2.2. Methods

The surface reactivity of the $BaTiO_3$ particles is insufficient for effective bonding with the PBAT matrix. Therefore, enhancing their surface properties is crucial to facilitate proper adhesion to the PBAT matrix. To address this issue, adipic acid was introduced, and tetrabutoxytitanium was employed as catalysts. Initially, adipic acid was dissolved in acetone, and $BaTiO_3$ particles were introduced into the solution. The resulting mixture was placed in an oil bath at 65 °C while

stirring, and tetrabutoxy titanium was added to serve as a catalyst, promoting interaction between $BaTiO_3$ particles and adipic acid, and the treatment was continued for 24 h. A 3 wt% concentration of adipic acid was used for treating the surface of $BaTiO_3$ particles. Adipic acid was chosen because it is a monomer in the PBAT polymer matrix, which aids in enhancing the surface morphology by reacting with the PBAT chains. The surface modification process is demonstrated in Fig. 1 (a).

In addition, the MWCNTs were subjected to oxalic anhydrous treatment in acetone to attach carboxylic groups to the MWCNT surface. Anhydrous oxalic acid treatment was performed in an oil bath with stirring at 80 °C for 4 h. Once the carboxylic attachment was completed, 5 wt% BD was supplied to the solution upon stirring. The mixture was stirred for 24 h and then subjected to vacuum filtration to separate MWCNTs from the solvent. The filter cake was dried in an oven for 24 h at 60 °C. BD is also a monomer of PBAT, which implies that treatment of the MWCNT surface with BD enhances the interaction between PBAT and the filler. Fig. 1 (b) shows the surface modification of MWCNTs with BD.

To prepare the composites, a constant 3 wt% MWCNT was used, and the amount of $BaTiO_3$ was varied to evaluate its effect. Slow-speed melt blending technique was used to fabricate the composite materials at the processing temperature of 140 °C. The extrusion speed was lowered to control the viscosity in order to prevent processing hindrance. Four composite samples were prepared by varying the $BaTiO_3$ particle content while keeping the MWCNT content constant at 3 wt%: 10, 20, 30, and 40 wt% of $BaTiO_3$ particles +3 wt% MWCNTs for each, one with 40 wt% $BaTiO_3$ particles and another one with only 3 wt% MWCNT composites. After obtaining the melt-blended composites, the specimens were injection-molded to obtain specific products for analysis, dog-bone shaped and circular disks. During injection molding, neat PBAT was also molded for comparison with the fabricated composites at medium injection and rotor speeds. Thus, the samples were designated as PBAT, BT, CNT, 10, 20, 30, and 40, representing the neat PBAT (40 wt% $BaTiO_3$ particles-PBAT, 3 wt% MWCNT-PBAT, (10, 20, 30, 40 wt% $BaTiO_3$ particles) + 3 wt% MWCNT-PBAT polymer matrix, respectively. This study aims to investigate the influence of varying the filler content and surface treatment on the mechanical properties of composite materials. Based on this comprehensive analysis, it is anticipated that the developed composites will exhibit improved mechanical characteristics compared to those of neat polymers, making them promising candidates for various engineering applications.

2.3. Characterization

Surface modifications of the $BaTiO_3$ and MWCNT particles through adipic acid and BD attachment, respectively, were analyzed using Fourier-transform infrared (FTIR) spectroscopy (Nicolet, IS5, Thermo Fisher Scientific, Seoul, Korea). The surface morphologies of the adipic acid-treated $BaTiO_3$ particles and BD-treated MWCNT particles, along with the various polymer composites, were investigated using field emission scanning electron microscopy (FE-SEM; Sigma, Carl Zeiss, Oberkochen, Germany) after fracturing each specimen with liquid nitrogen and applying a Pt coating to prevent charging. The quantities of BD and adipic acid groups attached to the MWCNT and $BaTiO_3$ particles were determined using thermogravimetric analysis (TGA, TGA-2050, TA Instruments, New Castle, DE, USA) and X-ray photoelectron spectroscopy (XPS; K-Alpha, Thermo Fisher Scientific). In addition, the thermogravimetric properties of neat PBAT, PBAT-MWCNT blend, and various (MWCNT-$BaTiO_3$)-PBAT composites were investigated in the temperature range of 30–600 °C under a nitrogen gas atmosphere to prevent further oxidation.

The mechanical properties of the fabricated composite materials, including the tensile strength and elongation at the breaking point, were analyzed using a universal testing machine (UTM; model UTM-301, R&B Corp., Daejeon, Korea) according to the ASTM D412 standards at room temperature, with a cross-head speed of 10 mm/min and a loading force
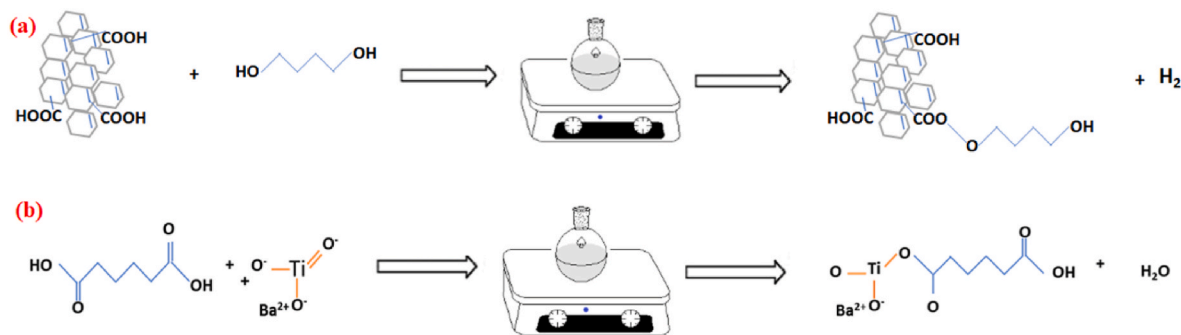
Fig. 1. (a) Surface treatment of MWCNT with butanediol and (b) Surface modification of BaTiO$_3$ particles with adipic acid.

of 1 kN. Dog-bone-shaped melt-extruded specimens were prepared using a mini-molding machine,. The average tensile strength and elongation values at the breaking point were determined for three specimens of each sample.

Thermomechanical properties of the composite materials were studied by dynamic mechanical analysis (DMA 8000, PerkinElmer, USA) in the temperature range of −70 to 130 °C. The analysis was conducted with pressurized liquid nitrogen to achieve −70 °C, followed by a heating rate of 3 °C/min.

The dielectric properties of the composite materials were studied using an impedance analyzer (Agilent, 4294 A) in the frequency range of 40–10^7 Hz. In addition, the thermal conductivities of the composites at room temperature were determined using laser flash analysis (LFA467 Hyper-Flash, Netzsch Instrument Co., Selb, Germany) by preparing circular specimens with a thickness of 1.4 mm and a diameter of 10 mm.

Finally, we conducted additional investigations using the Underwriters Laboratory (UL94-V) test to analyze the fire-resistance mechanisms. This involved subjecting the 130 × 13 × 3 mm^3 composite samples to direct flame for a specific duration.

3. Results and discussion

Harnessing the synergistic effects of BaTiO$_3$ and MWCNTs, coupled with surface improvements, is essential for achieving significant enhancements in the key properties of PBAT composites, thereby facilitating the development of high-performance materials suitable for various electronic applications.

In this study, we investigated the effects of BD treatment on MWCNTs and adipic acid treatment of BaTiO$_3$ particles using various analytical techniques. We employed TGA, FE-SEM, and FTIR spectroscopy to study the chemical and physical changes in the particles after BD treatment. In addition, we analyzed the adipic acid treatment of the BaTiO$_3$ particles using XPS to investigate whether the carbon group arising from adipic acid was available on the BaTiO$_3$ particle surface.

FTIR spectroscopy of the BD-treated MWCNT particles (Fig. 2(a)) revealed the presence of hydroxyl, methylene, and carbonyl groups on the particle surfaces, as evidenced by peaks at 3440, 2950, and 1100 cm^{-1}, respectively. These functional groups originate from the BD molecules that contain hydroxyl, methylene, and carbonyl groups from
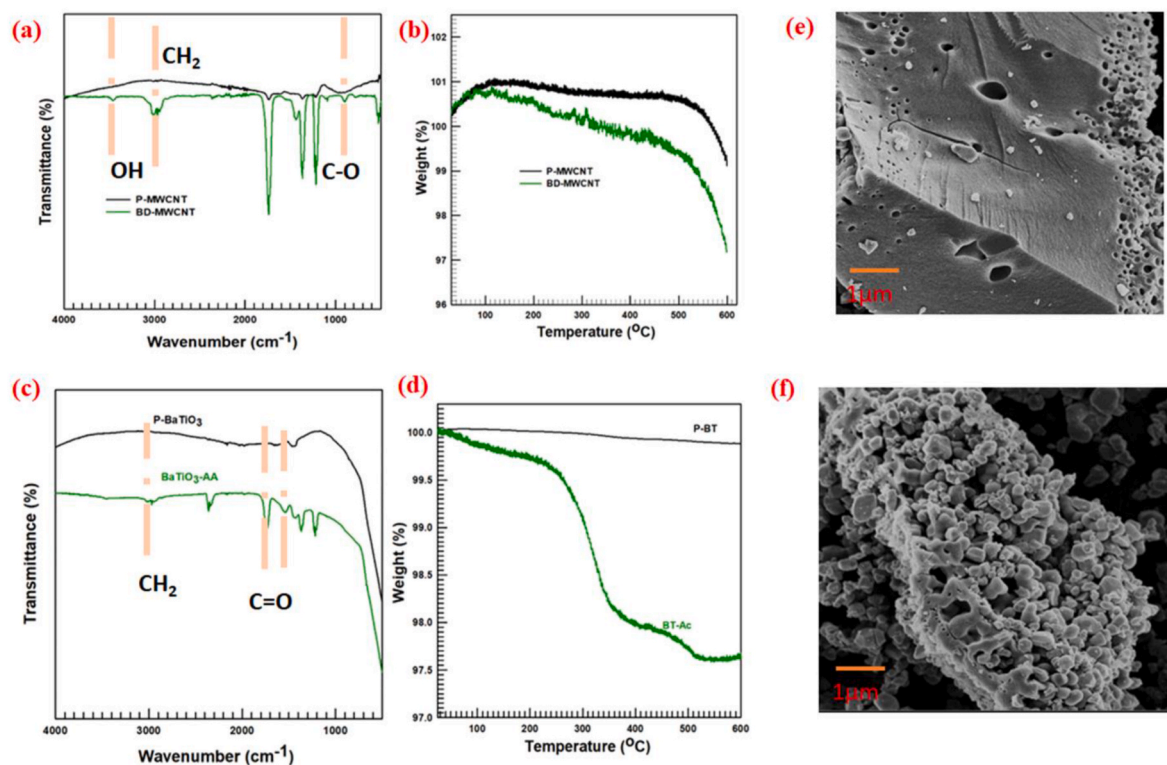

Fig. 2. Characterization of surface treatment of MWCNT and BaTiO$_3$ particles: (a) and (b) FTIR investigation and TGA of BD modified MWCNTs respectively; (c) and (d) FTIR and TGA investigation of adipic acid modified BaTiO$_3$ particles respectively; and (e) and (f) are morphological investigation of pristine and adipic-acid-treated BaTiO$_3$ particles respectively.

the addition of oxalic acid to the surface of the MWCNTs. The FTIR investigation Similarly, the FTIR spectra of the adipic acid-treated BaTiO$_3$ particles (Fig. 2(c)) exhibited distinct peaks corresponding to methylene, carbonyl, and C–O groups at 2950, 1660, and 1380 cm^{-1}, respectively. These functional groups arise from adipic acid groups.

The FE-SEM images of the pristine BaTiO$_3$ particles and adipic-acid-treated BaTiO$_3$ particles are shown in Fig. 2 (e and f). A smooth surface was observed for the pristine BaTiO$_3$ particles (Fig. 2(e)), whereas adipic acid was distributed over the surfaces of the BaTiO$_3$ particles, as shown in Fig. 2(f). The evenly distributed particles in Fig. 2(f) were considered adipic acid molecules, which details the treatment of BaTiO$_3$ particles.

The TGA results for the BD-MWCNT and adipic acid-BaTiO$_3$ particles are shown in Fig. 2(b) and (2), respectively. The result in Fig. 2(b) indicates that the MWCNTs were thermally stable up to 480 °C, and after this temperature, some of the MWCNTs degraded. However, the BD-treated MWCNTs started degrading at 180 °C, at which the moistures degrade, and the butane groups started degrading. At temperatures >500 °C, ~3 wt% of MWCNTs degraded, corresponding to the amount of BD groups attached to the surface of the MWCNTs to modify their surface. Similarly, a TGA investigation of adipic acid-treated BaTiO$_3$ particles was performed compared to pristine BaTiO$_3$ particles (Fig. 2 (d)). The pristine BaTiO$_3$ particles exhibited a highly thermally stable region even at higher temperatures, and no degradation was observed. However, as expected, the adipic acid-treated BaTiO$_3$ particles started degradation at lower temperatures and continued until 550 °C, the temperature at which the reacted adipic acid groups completely degraded, and the remaining residue is considered BaTiO$_3$ particles. Approximately 2.5 wt% of the total weight was degraded, which stipulates that the adipic acid attached to the surface BaTiO$_3$ particles was 2.5 wt%, and the rest 2.5 wt% was unreacted as 5 wt% adipic acid was used in the surface treatment of the BaTiO$_3$ particles in the previously conducted analysis.

Furthermore, XPS analysis is employed to distinguish the elemental composition of the pristine BaTiO$_3$ particles and BaTiO$_3$ particles treated with adipic acid molecules. Prior to XPS analysis, the particles are subjected to drying to prevent moisture disturbance during analysis. The outcomes of the XPS analysis are depicted in Fig. 3. Broader survey scans of XPS analysis for both pristine and adipic acid-functionalized BaTiO$_3$ particles are presented in Fig. 3(a). The binding energy of 285 eV is attributed to C1s originating from the adipic acid introduced during the surface functionalization of BaTiO$_3$ particles.

To further examine whether the XPS spectra depict the surface modification of BaTiO$_3$ particles with adipic acid molecules as compared to pristine BaTiO$_3$ particles Gaussian fitting was employed for deconvolution. The deconvolution results for adipic acid treated BaTiO$_3$ particles are presented in Fig. 3(b, c and d). In addition, Table 1 shows an increase in the atomic percentage of carbon atom in the adipic acid treated BaTiO$_3$ particles as compared to pristine BaTiO$_3$ particles. The atomic percentage of C1s increased from 25.14 (pristine BaTiO$_3$ particles) to 42.25 wt% (adipic acid treated BaTiO$_3$ particles) which is due to the attachment of adipic acid to the BaTiO$_3$ particles. In addition a drop in the atomic percentage of Ba3d, Ti2p and O1s is observed for the adipic acid treated BaTiO$_3$ particles, which might be due to the occupation of the area by C1s arising from adipic acid.

The FE-SEM images in Fig. 4 (a and b) reveal the surface morphologies of the various fractured specimens. The neat PBAT exhibited a fractured ladder-like morphology, suggesting a ductile nature (Figure a).

Table 1
Atomic percentage of pristine and adipic acid treated BaTiO$_3$ particles.

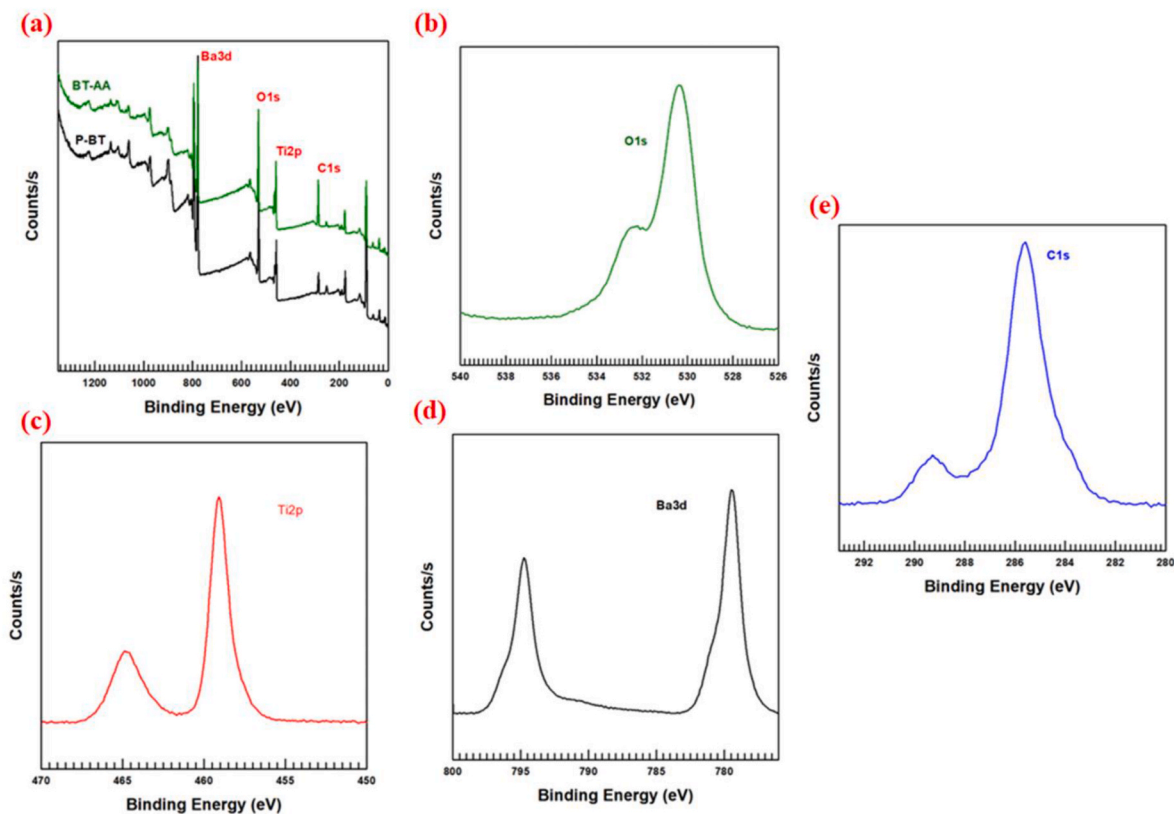| Name	Atomic % (PBT)	Atomic % (BT-AA)
Ba3d	16.39	7.53
O1s	45.96	39.58
Ti2p	12.51	10.64
C1s	25.14	42.25

Fig. 3. XPS investigation: (a) Survey scan of pristine and adipic acid treated BaTiO$_3$ particles; (b, c, d, and e) Deconvoluted peaks of O1s, Ti2p, Ba3d and C1s of adipic acid treated BaTiO$_3$ particles respectively.
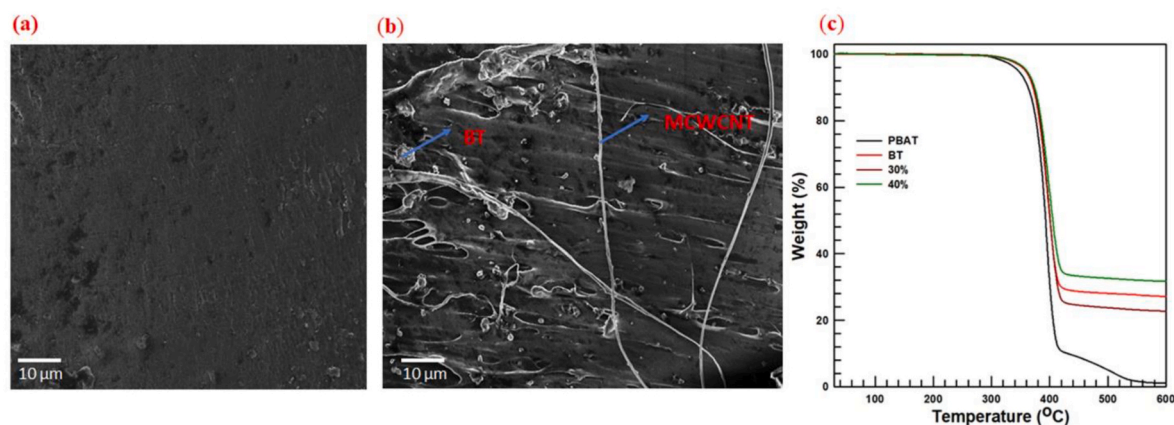
Fig. 4. (a) FE-SEM images of pristine PBAT; (b) PBAT with 30 wt% of BaTiO$_3$ particles and MWCNT and (c) TGA analysis.

The FE-SEM image in Fig. 4 (b) reveals that the adipic-acid-modified BaTiO$_3$ particles and BD-treated MWCNT were well distributed in the PBAT matrix. This demonstrates good interfacial adhesion between the filler particles and PBAT blend because of the compatibilizing nature of the adipic acid treatment and reaction between the BD molecules and PBAT soft segments.

The TGA results of the PBAT composites are shown in Fig. 4 (c). Compared to neat PBAT, the thermal stability of the PBAT-MWCNT composite was enhanced by the addition of BD-treated MWCNTs and adipic acid-modified BaTiO$_3$ particles. The neat PBAT displays two thermal degradation regions: (i) degradation of the BD segments in PBAT, starting at 380 °C, continuing linearly up to 410 °C, and completing at 415 °C; (ii) degradation of adipic acids in PBAT, starting at 420 °C and continuing linearly up to 425 °C, with <1 wt% residues remaining. Therefore, PBAT is a thermally stable polymer. Similarly, the BD-MWCNT-adipic acid-BaTiO$_3$-PBAT composites exhibit two-stage thermal degradation: (i) degradation of the adipic acid chain of PBAT, with immediate effect at 370 °C; (ii) degradation of the remaining segments, along with complete degradation of BD and adipic acid groups, between 380 and 420 °C;, with the remaining residues being MWCNTs and BaTiO$_3$ particles. The thermal stability of PBAT was superior to the other components, which is attributed to its higher glass transition temperature, as discussed in the DMA investigation. This indicates PBAT is more resistant to degradation or deformation when subjected to greater heat. The degradation patterns of the specimens considered is summarized in Table 2. The thermal degradation regions for various composites, particularly in the residue region, varied based on the inclusion of the filler material weight percentages within the PBAT matrix.

The mechanical properties of the various PBAT composites were elucidated using the UTM results, as shown in Fig. 5. The average tensile strength of neat PBAT was ~5.6 MPa. The tensile strength increased (displaying a maximum point) upon including adipic-acid-treated BaTiO$_3$ particles, reaching ~7.4 MPa (Fig. 5 (a)). By comparison, the PBAT-MWCNT polymer blend exhibits a tensile strength of 5.2 MPa, the lowest of all the specimens. The tensile strength of the PBAT-CNT composites improved with the addition of BaTiO$_3$ particles. The strength at break increased proportionally with the loading percentage of BaTiO$_3$ particles added to the matrix. 40 showed the highest (~7.0) strength at break, but this value was lower than that of BT. Thus, the insertion of MWCNTs deteriorated the mechanical properties, whereas including BaTiO$_3$ particles improved the strength at the breakpoint. Moreover, the elongation at break was not adversely affected by adding the MWCNTs or BaTiO$_3$ particles, as shown in Fig. 5 (b). The elongation at break for the MWCNT composite displayed a slight drop compared to the performance of the other specimens, which is owing to the nature of MWCNTs and poor mechanical properties of carbon materials.

The dynamic mechanical analysis (DMA) results in Fig. 6 provide insights into the thermomechanical properties of various (BD-treated MWCNTs and adipic acid-modified BaTiO$_3$)-PBAT composites. The storage modulus reflects the stiffness of each composite, and the glass transition temperature is represented by the tan δ value. As the loading percentage of the filler relative to the matrix increased, the storage modulus at low temperatures increased (Fig. 6 (a)). At room temperature, the storage modulus curve evolved from a concave downward trend to a concave upward trend, with 40 composites exhibiting the highest value. Fig. 6 (b) stipulates the glass transition temperatures of −20 °C for the neat PBAT, and the incorporation of the filler particles causes the curve of each composite to shift to the right, indicating a higher glass transition temperature compared to the neat PBAT. By contrast, the MWCNT composites demonstrate a shift towards the left, as shown by the arrow in Fig. 6 (b).

The charge storage capabilities of the various composites were revealed through the impedance characteristics shown in Fig. 7. Fig. 7 (a) shows the dielectric constant at variable frequencies in the range of 40–10^{7}Hz. At lower frequencies, neat PBAT samples demonstrated a poor dielectric constant of ~2; similarly, the MWCNT-PBAT (CNT) composites displayed a poor dielectric constant of ~3.5. Including BaTiO$_3$ particles significantly improved the dielectric constant; for BT, it became >43, approximately the same region as the 40 composites. As the frequency increases, the dielectric constant of each specimen decreases to a minimum and remains constant after that. Throughout the frequency range, neat PBAT exhibited the lowest dielectric constant, followed by the CNT composite and, finally, the 10 composites. The dielectric constants were determined at a constant frequency of 1 MHz. At 1 MHz frequency, PBAT exhibited the lowest value of 1.4, followed by that of the CNT composite, whereas the composites containing BaTiO$_3$ particles exhibited a higher dielectric constant. Forty composite specimens attained a dielectric constant of 27.5, which was 1800 % higher than that of the neat PBAT matrix. Thus, a composite with a very high dielectric constant was obtained upon the inclusion of 40 wt% BaTiO$_3$ particles and 3 wt% MWCNTs. Table.

The fire-resistance mechanisms of the composites were studied by analyzing their burning behavior using UL94-V testing. The images of the samples after the UL94-V test are shown in Fig. 8. When a flame was applied, the PBAT sample immediately emitted drips, indicating poor fire resistance. Furthermore, the CNT composites displayed a fast
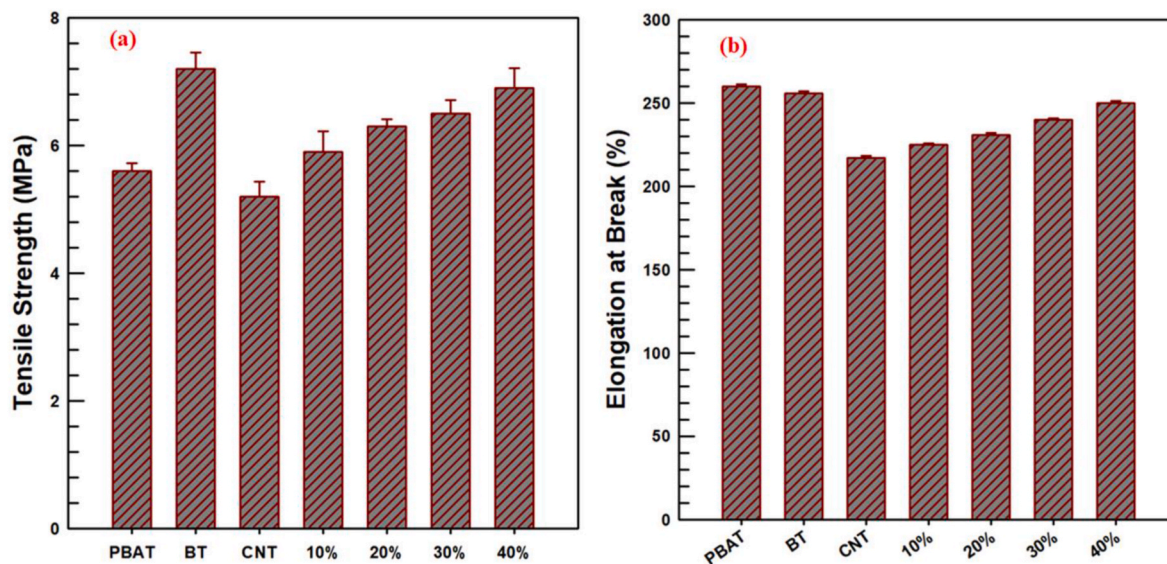
Table 2
Degradation stages of the composites.

Specimen	Initial degradation temperature (°C)	Final residue Temperature (°C)
PBAT	380	425
BT	370	420
30	365	419
40	368	420

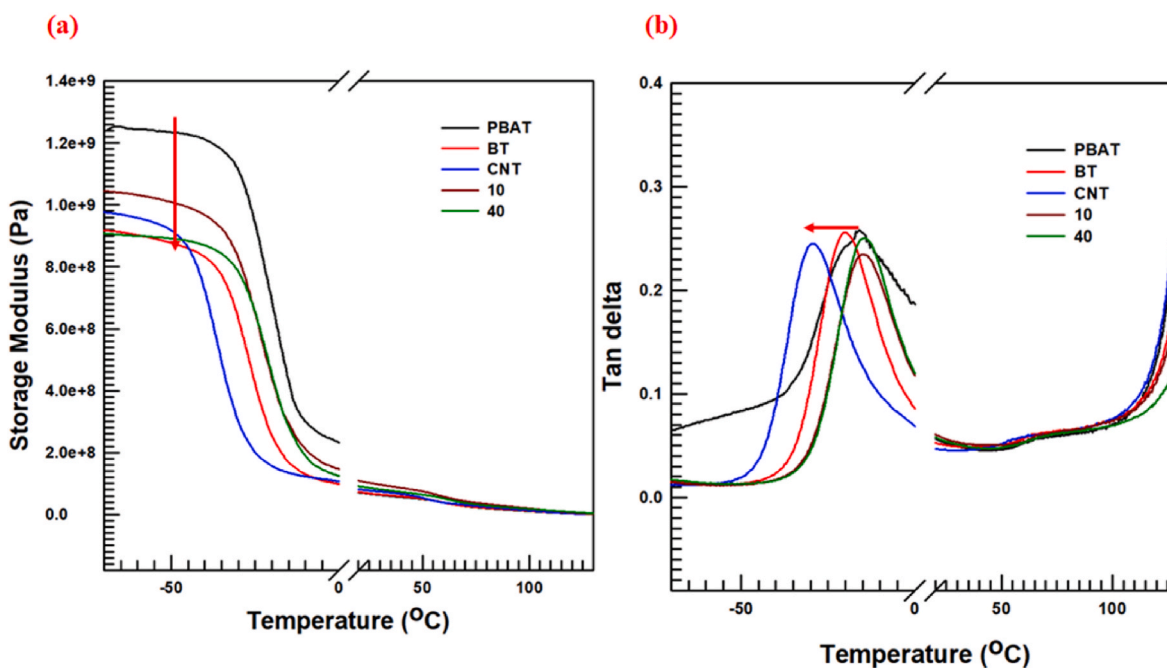**Fig. 5.** (a) Tensile strength and (b) Elongation at break.

Fig. 6. DMA: (a) Storage Modulus; and (b) tan δ

burning rate in a similar fashion but with a lower dripping rate compared to neat PBAT. Interestingly, the BT composites showed higher resistance to burning and almost no dripping rate, even after waiting for >15 s. Therefore, we concluded that the $BaTiO_3$ particles have a higher fire resistance property than the other composites in this study. However, including MWCNTs and $BaTiO_3$ in the PBAT composites caused the composite materials to burn but with a much lower dripping rate than the CNT-PBAT composites. Table 3 describes the dripping performance of the composites investigated by UL-94.

LFA was used to investigate the thermal conductivity of PBAT composite materials with adipic acid functionalized $BaTiO_3$ and butanediol treated MWCNT particles. Typical polymer materials exhibit notably low thermal conductivity values, generally below 0.2 W/(m·K). The thermal conductivity is typically influenced by factors such as filler alignment within the polymer matrix, polymer chain defects, and the presence of voids. The thermal conductivity (K) of composite materials is calculated using the relationship depicted in equation (1).

$$: K = \rho Cp\delta \qquad \text{equation 1}$$

The LFA machine determines the thermal diffusivity based on the thickness (1.43 mm) and diameter (10 mm) of the sample, while the values of Cp and ρ are obtained from differential scanning calorimetry and considering the particle as circular disks, respectively.

This study delves into the impact of incorporating adipic acid functionalized $BaTiO_3$ and butanediol treated MWCNT particles into PBAT polymer matrix on thermal conductivity. As the loading percentage of adipic acid functionalized $BaTiO_3$ and butanediol treated MWCNT particles increases, the thermal conductivity experiences a linear increase as shown in Fig. 9. With the addition of 40 wt% adipic acid functionalized $BaTiO_3$ and butanediol treated MWCNT particles into the PBAT
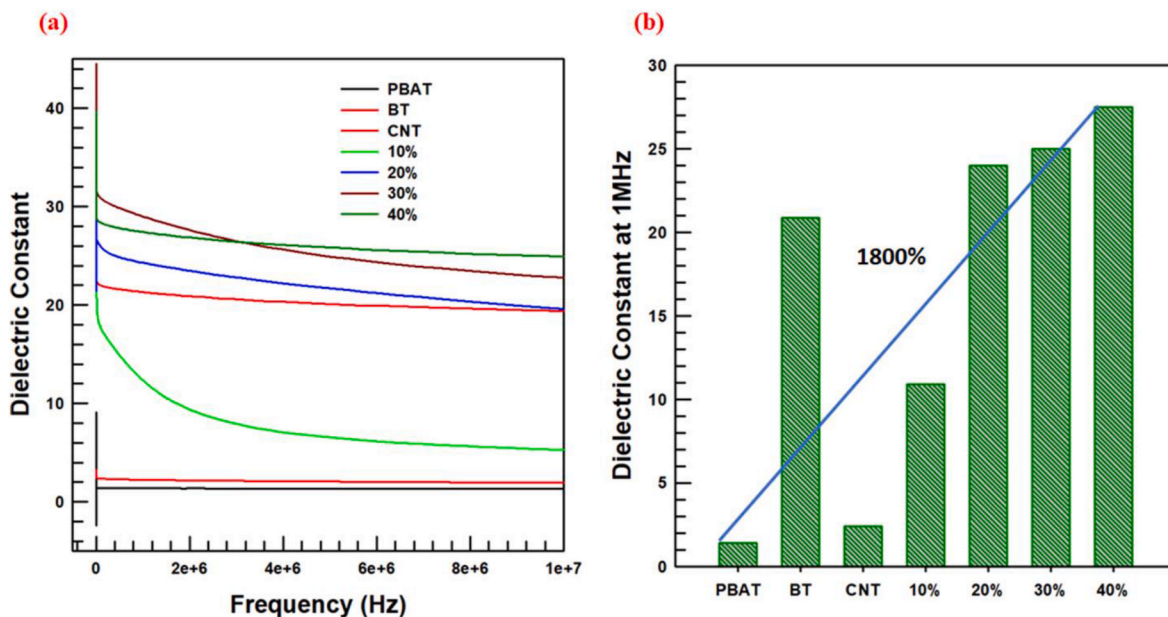
Fig. 7. (a) Dielectric constant at variable frequency; and (b) Dielectric constant at 1 MHz.
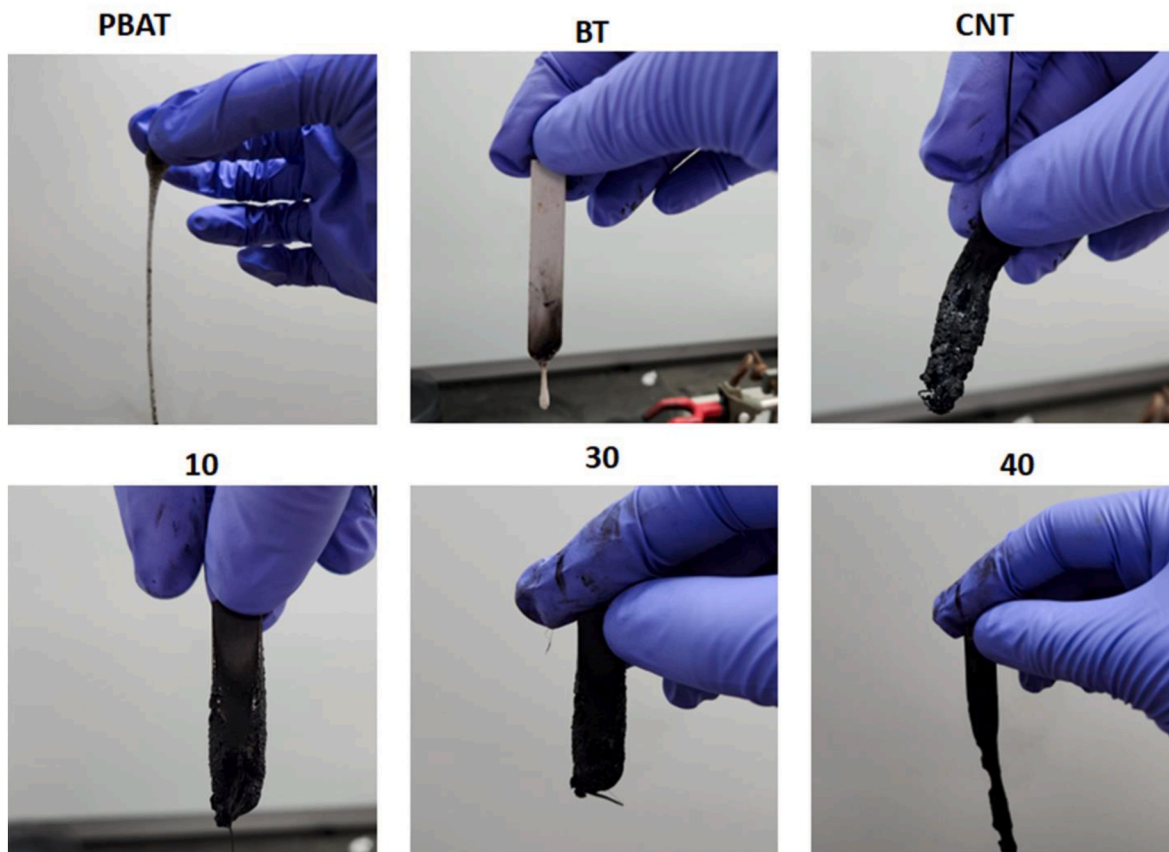

Fig. 8. Photographs of UL 94 results.

matrix, a remarkable enhancement of 245 % in thermal conductivity is achieved compared to the neat PBAT matrix. This enhancement can be attributed to the presence of 3 wt% MWCNT in conjunction with BaTiO$_3$ particles, summing up to a total filler content of 40 wt% relative to the polymer matrix. It can be observed in the figure that inclusion of 3 wt% of CNT has increased the thermal conductivity up to 0.92 W/(m.K)

which is 3.6 times of the neat PBAT. It was assumed to improve the thermal conductivity more however due to polymer chain defects it was hindered.

Table 3
UL-94 results dripping performance.

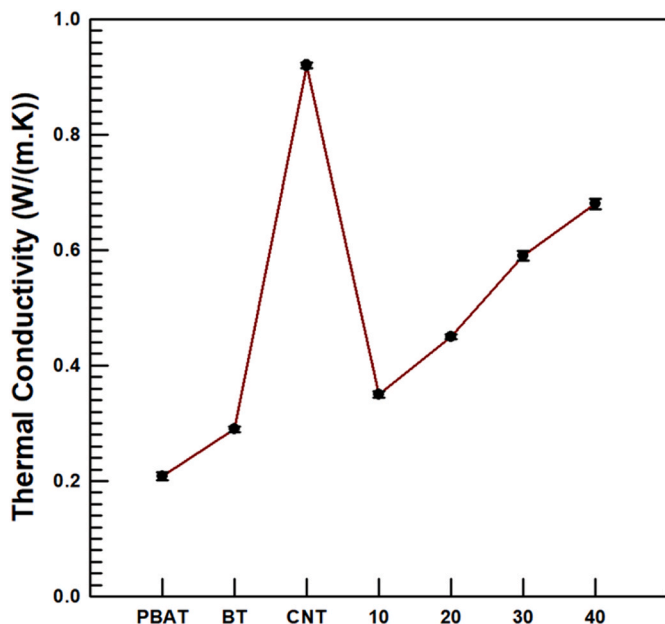| Sample	Dripping
PBAT	Yes
BT	No
CNT	Yes
10	Yes
20	Yes
30	Yes
40	Yes

Fig. 9. Thermal conductivity of the composites.

4. Conclusion

In this study, we aimed to enhance the dielectric properties and thermal conductivities of polymer blends containing PBAT by incorporating a suitable mixed filler. Mainly, $BaTiO_3$ particles were introduced to improve dielectric properties, whereas MWCNTs were used to enhance thermal conductivity. Hydroxylation was applied to the $BaTiO_3$ particles to activate surface reactivity, followed by functionalization with adipic acid (AA), which acted as a compatibilizer between the two polymer components in the matrix. Similarly, the MWCNT particles were hydroxylated and reacted with BD molecules, which subsequently reacted with the PBAT soft segments. The composites were prepared using a melt-blending technique and further analyzed for their morphologies, thermal stabilities, viscoelastic properties, tensile properties, thermal conductivities, and dielectric properties. The results revealed that the inclusion of BD-treated MWCNTs and AA-modified $BaTiO_3$ particles improved the thermal stability of the composite while retaining an increased tensile strength compared to that of neat PBAT; however, the composite containing only MWCNTs attained the lowest tensile strength and elongation at break. Furthermore, the dielectric constant of the 40 composites at 1 MHz displayed a remarkable 18-times increment compared with that of the PBAT matrix. In addition, the inclusion of BD-treated MWCNTs and AA-modified $BaTiO_3$ particles increased thermal conductivity. Adding $BaTiO_3$ particles also improved the fire resistance properties of the composite.

CRediT authorship contribution statement

Eyob Wondu: Writing – original draft, Methodology, Investigation,

Formal analysis, Conceptualization, Writing – review & editing. **Geun-hyeong Lee:** Data curation, Resources, Software, Visualization, Writing – review & editing. **Jooheon Kim:** Funding acquisition, Project administration, Supervision.

Declaration of competing interest

The authors declare that they have no known competing financial interests or personal relationships that could have appeared to influence the work reported in this paper.

Data availability

The data used in this research work is included in the manuscript.

References

[1] H. Chen, V.V. Ginzburg, J. Yang, Y. Yang, W. Liu, Y. Huang, L. Du, B. Chen, Thermal conductivity of polymer-based composites: fundamentals and applications, Prog. Polym. Sci. 59 (2016) 41–85, https://doi.org/10.1016/j.progpolymsci.2016.03.001.
[2] L. Variar, M.N. Muralidharan, S.K. Narayanankutty, S. Ansari, High dielectric constant and low-loss, carbon black/CaCu3Ti4O12/epoxy composites for embedded capacitor applications, Mater. Res. Bull. 152 (2022) 111835, https://doi.org/10.1016/j.materresbull.2022.111835.
[3] W. Zhou, Y. Kou, M. Yuan, B. Li, H. Cai, Z. Li, F. Chen, X. Liu, G. Wang, Q. Chen, Z.M. Dang, Polymer composites filled with core@double-shell structured fillers: effects of multiple shells on dielectric and thermal properties, Compos. Sci. Technol. 181 (2019), https://doi.org/10.1016/j.compscitech.2019.107686.
[4] S. Hong, C.S. Lee, M.H. Lee, Y. Lee, K.Y. Ma, G. Kim, S.I. Yoon, K. Ihm, K.J. Kim, T.J. Shin, S.W. Kim, E. chae Jeon, H. Jeon, J.Y. Kim, H.I. Lee, Z. Lee, A. Antidormi, S. Roche, M. Chhowalla, H.J. Shin, H.S. Shin, Ultralow-dielectric-constant amorphous boron nitride, Nature 582 (2020) 511–514, https://doi.org/10.1038/s41586-020-2375-9.
[5] E. Wondu, Z. Lule, J. Kim, Thermal conductivity and mechanical properties of thermoplastic polyurethane-/silane-modified Al2O3 composite fabricated via melt compounding, Polymers 11 (2019) 1103, https://doi.org/10.3390/polym11071103.
[6] X. Tan, Q. Yuan, M. Qiu, J. Yu, N. Jiang, C. Te Lin, W. Dai, Rational design of graphene/polymer composites with excellent electromagnetic interference shielding effectiveness and high thermal conductivity: a mini review, J. Mater. Sci. Technol. 117 (2022) 238–250, https://doi.org/10.1016/j.jmst.2021.10.052.
[7] K.W. Paik, J.G. Hyun, S. Lee, K.W. Jang, Epoxy/BaTiO3 (SrTiO3) composite films and pastes for high dielectric constant and low tolerance embedded capacitors in organic substrates, in: ESTC 2006 - 1st Electron. Syst. Technol. Conf., Institute of Electrical and Electronics Engineers Inc., 2006, pp. 794–801, https://doi.org/10.1109/ESTC.2006.280102.
[8] S. Kwon, W. Hackenberger, E. Alberta, E. Furman, M. Lanagan, Nonlinear dielectric ceramics and their applications to capacitors and tunable dielectrics, IEEE Electr. Insul. Mag. 27 (2011) 43–55, https://doi.org/10.1109/MEI.2011.5739422.
[9] L. Yao, Z. Pan, J. Zhai, G. Zhang, Z. Liu, Y. Liu, High-energy-density with polymer nanocomposites containing of SrTiO3 nanofibers for capacitor application, Composer Part A Appl. Sci. Manuf. 109 (2018) 48–54, https://doi.org/10.1016/j.compositesa.2018.02.040.
[10] L. Yao, Z. Pan, J. Zhai, G. Zhang, Z. Liu, Y. Liu, High-energy-density with polymer nanocomposites containing of SrTiO3 nanofibers for capacitor application, Composer Part A Appl. Sci. Manuf. 109 (2018) 48–54, https://doi.org/10.1016/j.compositesa.2018.02.040.
[11] J. Wang, Y. Long, Y. Sun, X. Zhang, H. Yang, B. Lin, Enhanced energy density and thermostability in polyimide nanocomposites containing core-shell structured BaTiO 3 @SiO 2 nanofibers, Appl. Surf. Sci. 426 (2017) 437–445, https://doi.org/10.1016/j.apsusc.2017.07.149.
[12] H. Ye, T. Lu, C. Xu, M. Zhong, L. Xu, Enhanced energy density and thermal conductivity in poly(fluorovinylidene-co-hexafluoropropylene) nanocomposites incorporated with boron nitride nanosheets exfoliated under assistance of

hyperbranched polyethylene, Nanotechnology 29 (2018), https://doi.org/10.1088/1361-6528/aaa318.

[13] J. Xiong, Z. Zheng, X. Qin, M. Li, H. Li, X. Wang, The thermal and mechanical properties of a polyurethane/multi-walled carbon nanotube composite, Carbon N. Y. 44 (2006) 2701–2707, https://doi.org/10.1016/j.carbon.2006.04.005.

[14] H.C. Kuan, C.C.M. Ma, W.P. Chang, S.M. Yuen, H.H. Wu, T.M. Lee, Synthesis, thermal, mechanical and rheological properties of multiwall carbon nanotube/waterborne polyurethane nanocomposite, Compos. Sci. Technol. 65 (2005) 1703–1710, https://doi.org/10.1016/j.compscitech.2005.02.017.

[15] H. Yu, P. Guo, M. Qin, G. Han, L. Chen, Y. Feng, W. Feng, Highly thermally conductive polymer composite enhanced by two-level adjustable boron nitride network with leaf venation structure, Compos. Sci. Technol. 222 (2022) 109406, https://doi.org/10.1016/j.compscitech.2022.109406.

[16] B. Liu, Y. Li, T. Fei, S. Han, C. Xia, Z. Shan, J. Jiang, Highly thermally conductive polystyrene/polypropylene/boron nitride composites with 3D segregated structure prepared by solution-mixing and hot-pressing method, Chem. Eng. J. 385 (2020), https://doi.org/10.1016/j.cej.2019.123829.

[17] Z. Lule, J. Kim, Thermally conductive and highly rigid polylactic acid (PLA) hybrid composite filled with surface treated alumina/nano-sized aluminum nitride, Composer Part A Appl. Sci. Manuf. 124 (2019), https://doi.org/10.1016/j.compositesa.2019.105506.

[18] D. Jayabalakrishnan, P. Prabhu, S. Mohamed Iqbal, V. Mugendiran, S. Ravi, V. R. Arun Prakash, Mechanical, dielectric, and hydrophobicity behavior of coconut shell biochar toughened Caryota urens natural fiber reinforced epoxy composite, Polym. Compos. 43 (2022) 493–502, https://doi.org/10.1002/pc.26393.

[19] C. Chen, Y. Tang, Y.S. Ye, Z. Xue, Y. Xue, X. Xie, Y.W. Mai, High-performance epoxy/silica coated silver nanowire composites as underfill material for electronic packaging, Compos. Sci. Technol. 105 (2014) 80–85, https://doi.org/10.1016/j.compscitech.2014.10.002.

[20] L. Zhao, Z. Chen, J. Ren, L. Yang, Y. Li, Z. Wang, W. Ning, S. Jia, Synchronously improved thermal conductivity and dielectric constant for epoxy composites by introducing functionalized silicon carbide nanoparticles and boron nitride microspheres, J. Colloid Interface Sci. 627 (2022) 205–214, https://doi.org/10.1016/j.jcis.2022.07.058.

[21] F.P. Du, J.J. Li, P. Fu, Y.G. Wu, G.Y. Liao, Y.F. Zhang, S. Luo, Enhanced thermal conductivity of poly(L-lactide) composites with synergistic effect of aluminum nitride and modified multi-walled carbon nanotubes, Fullerenes Nanotub, Carbon Nanostruct. 24 (2016) 667–673, https://doi.org/10.1080/1536383X.2016.1224236.

[22] A.S. Osipov, P. Klimczyk, P. Rutkowski, Y.A. Melniychuk, L.O. Romanko, M. Podsiadlo, I.A. Petrusha, L. Jaworska, Diamond composites of high thermal conductivity and low dielectric loss tangent, Mater. Sci. Eng. B 269 (2021) 115171, https://doi.org/10.1016/j.mseb.2021.115171.

[23] Q. Chi, X. Zhang, X. Wang, C. Zhang, Y. Zhang, C. Tang, Z. Li, T. Zhang, High thermal conductivity of epoxy-based composites utilizing 3D porous boron nitride framework, Compos. Commun. 33 (2022) 101195, https://doi.org/10.1016/j.coco.2022.101195.

[24] S. Wang, Y. Liu, Y. Guo, Y. Lu, Y. Huang, H. Xu, D. Wu, J. Sun, Optimal analysis for thermal conductivity variation of EVA/SCF composites prepared by spatial confining forced network assembly, Mater. Today Commun. 25 (2020) 101206, https://doi.org/10.1016/j.mtcomm.2020.101206.

[25] E. Wondu, Z.C. Lule, J. Kim, Fabrication of high dielectric properties and higher thermal conductivity thermoplastic polyurethane composites with CNT-covered SrTiO3, Polym. Test. 110 (2022) 107576, https://doi.org/10.1016/j.polymertesting.2022.107576.

[26] J. Meng, P. Chen, R. Yang, L. Dai, C. Yao, Z. Fang, K. Guo, Thermal stable honokiol-derived epoxy resin with reinforced thermal conductivity, dielectric properties and flame resistance, Chem. Eng. J. 412 (2021) 128647, https://doi.org/10.1016/j.cej.2021.128647.

[27] T.A. Taha, M.A.A. Alzara, Synthesis, thermal and dielectric performance of PVA-SrTiO3 polymer nanocomposites, J. Mol. Struct. 1238 (2021), https://doi.org/10.1016/j.molstruc.2021.130401.

[28] W. Wang, K. Meng, P.Z. Ge, X.G. Tang, Q.X. Liu, Y.P. Jiang, Paraelectric matrix-tuned energy storage in BiFeO3-BaTiO3-SrTiO3Relaxor ferroelectrics, ACS Appl. Energy Mater. 4 (2021) 9216–9226, https://doi.org/10.1021/acsaem.1c01474.

[29] M. Cao, X.J. Yan, L. Li, S.Y. Wu, X.M. Chen, Obtaining greatly improved dielectric constant in BaTiO3-epoxy composites with low ceramic volume fraction by enhancing the connectivity of ceramic phase, ACS Appl. Mater. Interfaces 14 (2022) 7039–7051, https://doi.org/10.1021/acsami.1c25069.

[30] X. Zhu, J. Yang, D. Dastan, H. Garmestani, R. Fan, Z. Shi, Fabrication of core-shell structured Ni@BaTiO3 scaffolds for polymer composites with ultrahigh dielectric constant and low loss, Composer Part A Appl. Sci. Manuf. 125 (2019), https://doi.org/10.1016/j.compositesa.2019.105521.

[31] X. Yin, Y. Luo, J. Zhang, Synthesis and characterization of halogen-free flame retardant two-component waterborne polyurethane by different modification, Ind. Eng. Chem. Res. 56 (2017) 1791–1802, https://doi.org/10.1021/acs.iecr.6b04452.

[32] Z.C. Lule, E. Wondu, J. Kim, Highly rigid, fire-resistant, and sustainable polybutylene adipate terephthalate/polybutylene succinate composites reinforced with surface-treated coffee husks, J. Clean. Prod. 315 (2021) 128095, https://doi.org/10.1016/j.jclepro.2021.128095.

[33] H. Zhu, S.A. Xu, Preparation and fire behavior of rigid polyurethane foams synthesized from modified urea-melamine-formaldehyde resins, RSC Adv. 8 (2018) 17879–17887, https://doi.org/10.1039/c8ra01846d.

[34] S. Kashi, R.K. Gupta, T. Baum, N. Kao, S.N. Bhattacharya, Dielectric properties and electromagnetic interference shielding effectiveness of graphene-based biodegradable nanocomposites, Mater. Des. 109 (2016) 68–78, https://doi.org/10.1016/j.matdes.2016.07.062.

[35] J. Guo, P. Saha, J. Liang, M. Saha, B.P. Grady, Multi-walled carbon nanotubes coated by multi-layer silica for improving thermal conductivity of polymer composites, J. Therm. Anal. Calorim. (2013) 467–474, https://doi.org/10.1007/s10973-012-2902-5.

[36] R. Han, Y. Liu, J. Shi, G.X. Chen, Q. Li, Enhanced dielectric properties and breakdown strength of polymer/carbon nanotube composites by coating an SrTiO3layer, E-Polymers 21 (2021) 272–278, https://doi.org/10.1515/epoly-2021-0028.